The following article appeared in Carbon, 149: 722-732 (2019) and may be found at: https://doi.org/10.1016/j.carbon.2019.04.109

Carbon 149 (2019) 722–732

Contents lists available at ScienceDirect

Carbon

journal homepage: www.elsevier.com/locate/carbon

Influence of protons on reduction degree and defect formation in electrochemically reduced graphene oxide

Javier A. Quezada-Renteria [a], Conchi O. Ania [b], Luis F. Chazaro-Ruiz [a, **], Jose R. Rangel-Mendez [a, *]

[a] División de Ciencias Ambientales, Instituto Potosino de Investigación Científica y Tecnológica A.C., Camino a la Presa San José 2055, Col. Lomas 4ª Sección, C.P., 78216, San Luis Potosí, SLP, Mexico
[b] POR2E Group, CEMHTI, CNRS (UPR 3079), Univ. Orleans, Orléans, 45071, France

ARTICLE INFO

Article history:
Received 21 March 2019
Received in revised form
25 April 2019
Accepted 27 April 2019
Available online 29 April 2019

Keywords:
Graphene oxide
Electrochemical reduction
Reduced graphene oxide
Defects

ABSTRACT

The electrochemical reduction of GO was investigated in aqueous, at both acid and basic pH, and organic media, to identify the possible role of protons (H^+) in the reduction mechanism of this material. The obtained rGO films were characterized by FTIR, electrochemical methods, Raman and XPS spectroscopy. Data showed that the reduction was more efficient in acid and basic media due to the presence of protons and the capacity of water that works as a proton donor, resulting in C/O ratios of 3.8 and 7.8, respectively. Mostly hydroxyl, epoxide and carbonyl moieties were removed. In a proton-free organic electrolyte, a C/O ratio of 1.8 was obtained for most of the samples; nevertheless, the graphitic carbon sp^2 domains were restored to a large extent in the absence of H^+. The characterization of the material showed that the presence of protons, during the electrochemical reduction, caused hydrogenation reactions, which targeted the graphitic domains in rGO and resulted in the loss of sp^2 hybridization. The presence of such defects modified the electrochemical properties of the rGO films, where, despite of exhibiting higher C/O ratio, the films reduced in aqueous electrolytes displayed lower electron transfer (e.g. ferrocyanide redox-probe) than those reduced in organic electrolyte.

1. Introduction

The oxidized form of graphene, graphene oxide (GO), has received a lot of attention for its technological implementation due to its unique properties such as hydrophilic character, tunable optical band gap, and high chemical reactivity, which are granted by the presence of the oxygen-containing functional groups in the 2D-carbon matrix [1]. These oxygenated groups can be removed using several methodologies to obtain reduced or partially reduced graphene oxide (rGO), a material with intermediate properties compared to GO and pristine graphene, and that offers interesting perspectives in many application fields [2]. Depending on the methodology applied, not only specific groups of GO can be removed, but also different defects are produced in the material. For instance, it is well accepted that the thermal reduction of GO are effective means to remove oxygen-containing surface groups in the form of CO_2, leading to the formation of holes or vacancies on the basal planes of the graphene sheets. This increases the number of edge-like zones and, thus, the chemical reactivity of the obtained rGO material [3–7]. On the other hand the chemical reduction of GO using hydrazine may yield a rGO with a certain degree of nitrogen functionalization [8]. Defects have a crucial role in the performance of rGO in an intended application, they bring to the table new chemical properties on the final material that may be, most of the times, undesired. Knowledge on the mechanism for the removal of surface groups and identification of the defects created in the rGO still remain quite uncertain and need to be addressed to define the specific features of the material.

Among the different procedures for the removal of oxygen groups (*e.g.*, chemical [2,9], thermal [5,10] and electrochemical [11,12]), the electrochemical reduction of GO is a simple approach that avoids both the use of hazardous chemical agents and elevated temperatures. It has been widely addressed in the literature, and often performed by cyclic voltammetry or chronoamperometry techniques applying potentials ranging from −0.6 to −1.5 V (*vs* Ag/

* Corresponding author.
** Corresponding author.
E-mail addresses: luis.chazaro@ipicyt.edu.mx (L.F. Chazaro-Ruiz), rene@ipicyt.edu.mx (J.R. Rangel-Mendez).

https://doi.org/10.1016/j.carbon.2019.04.109

AgCl), both in aqueous and organic media [11,13–15].

Most of the studies on the electrochemical reduction of GO report the preferential removal of epoxides, phenolic and carbonyl groups [11], while the carboxylic groups seem to remain mostly unaffected. It also has been observed that evolution of epoxide groups to phenolic or aldehyde moieties is dependent upon the pH of the electrolytic medium [13,16]. Data has suggested that the electrochemical potential needed for the reduction of GO decreases with the acidity of the electrolyte [17], making evident the role of H^+ in the removal of O-groups. In a proton-free organic electrolytic medium, the electrochemical reduction has been reported to occur in the potential range between −0.1 and −1.1 V (*vs* Ag/AgCl/NaCl 3 M), reaching a C/O ratio similar to that obtained in aqueous electrolytes [13]. No significant chemical and structural changes were reported at more cathodic potentials (as inferred from FTIR and Raman spectroscopies) [18]. As the electrochemical reduction of GO can be achieved in proton-free media (*e.g.*, organic electrolyte, and alkaline aqueous electrolyte), the exact role of protons still remains rather unclear [13,19,20]. Additionally, while most works focus on the identification of the O-groups removed/transformed upon the electrochemical reduction in different electrolytes, scarce information is available about the defects introduced in the graphene sheets during the electrochemical reaction. These aspects are important to point out and characterize, since there are important structural differences between the rGO materials obtained electrochemically (*i.e.*, defects introduced during the reduction) and pristine graphene that have been neglected [21,22].

In this work, we have investigated the electrochemical reduction of GO films in aqueous and organic electrolytes containing different proton concentrations, aiming to clarify the role of H^+ in the reduction reaction, and to determinate the nature and density of the defects introduced in the graphene sheets during their reduction. The latter could allow to identify how these defects affect the properties of the resulting rGO material.

2. Experimental section

2.1. Substances and materials

A commercial suspension of GO in water from Graphene Supermarket (*ca.* 6.2 g L^{-1}) was used to prepare all the electrodes evaluated in this work. According to the manufacturer it is a single-layer graphene oxide (at least 60%) produced by Hummer's method, with a composition of 79% C and 20% O. A complete characterization of this GO has been reported before [23]. All the aqueous solutions were prepared with deionized water with a resistivity of 18 MΩ cm. Phosphate salts, K_2HPO_4 and KH_2PO_4 (Fermont), were used as received to prepare a 0.1 M buffer solution (PBS), whose pH was adjusted to either 2 or 12 with H_3PO_4 (Fermont) or KOH (Sigma-Aldrich), respectively. The organic electrolyte was a solution of 0.1 M Tetrabutylammonium hexafluorophosphate (Sigma-Aldrich) in Acetonitrile (Baker, HPLC grade). The organic solvent was previously dehydrated with a molecular sieve for at least 24 h before use. Phthalic acid (Sigma-Aldrich) was added as a H^+ donor to the organic electrolytic solution in different concentrations. The organic salts were dried at 70 °C for at least 24 h before use.

2.2. Electrochemical reduction of GO electrodes

GO films were produced via drop-coating over a carbon steel substrate (AISI 1045). Before this, the carbon steel substrates were polished with silicon carbide papers starting from 200 up to 2000, then, the pieces of steel were cleaned in an ultrasonic bath using ethanol, and finally rinsed with a mixture of ethanol/acetone. Then, 100 μL of the GO suspension were dropped on the substrate and allowed to dry at room temperature (equivalent to 0.62 mg of GO); the obtained electrodes were stored in a desiccator until use. The electrochemical reduction was carried out using a three-electrode configuration cell, using the GO-coated carbon steel as working electrode, a platinum mesh as counter electrode and as reference electrodes, either, Ag/AgCl/NaCl 3 M or Ag/Ag^+ TBAP 0.1 M in acetonitrile (ACN) for aqueous and organic media, respectively. For the sake of clarity, all the potentials reported in this work will be referred to the Ag/AgCl/NaCl 3 M reference system. The electrochemical reduction was made using either cyclic voltammetry (*ca.* 15 scans) or chronoamperometry at different potential values between −0.8 and −1.5 V, and times ranging between 15 and 60 min. The latter experiments were conducted in a potentiostat/galvanostat model VMP3 Bio-Logic SAS controlled by the EC-Lab software version 10.23. After the electrochemical reduction, the obtained electrodes (now labelled as rGO) were mechanically detached from the substrate by pulling the films using stainless steel tweezers, then rinsed in water or ACN (depending on the electrolyte where they were reduced) and stored in a desiccator until characterization.

2.3. Characterization techniques

Raman spectra were obtained in a Renishaw Invia Raman Microscope, equipped with a 532 nm wavelength laser and a 100× objective. The laser was kept at 10% power and a 15 s exposition time was employed. FTIR spectra were recorded in a Thermo Scientific Nicolet 6700 FTIR. The samples (GO or rGO) were mixed with KBr (ratio sample:KBr of 0.46:99.54) and pressed to conform a 1 cm^2 pellet. The spectra were obtained after compilation of 64 scans at a resolution of 8 cm^{-1}. X-ray photoelectronic spectroscopy (XPS) experiments were collected in a PHI 5000 VersaProbe II system from Physical Electronics, using monochromatic Al-Kα (1486.6 eV) radiation and a charge neutralizing system. Spectra of dried samples were recorded using a 100 μm beam size, operating at 25 W and 15 KV. The high definition spectra were obtained using a pass energy of 23.5 eV and a 0.2 eV step size for 50 sweeps. The processing of the XPS spectra was performed using energy values referenced to the C 1s peak of adventitious carbon located at 284.6 eV, and a Shirley-type background. The deconvolution was done using the AAnalyzer software and the peak fitting was performed according to the Thermo scientific XPS database [24].

The electrochemical characterization of the materials was carried out by cyclic voltammetry in the presence of the ferrocyanide/ferricyanide couple. To conduct these experiments, the GO films were casted on a gold current collector, following the same protocol indicated above. The voltammogram was obtained at a scan rate of 20 mV s^{-1} using a 0.01 M $K_4[Fe(CN)_6]$ in 0.1 M PBS solution. The capacitance of the electrodes was measured in 0.5 M Na_2SO_4 at a scan rate of 10 mV s^{-1}. All the electrochemical tests (*i.e.* electrochemical reduction, capacitance and ferrocyanide/ferricyanide probe) were performed at least three times to assure reproducibility; a standard deviation below *ca.* 7% was found (differences are most certainly caused by the mass variation of the electrodes due to the assembling of the films by drop coating).

3. Results and discussion

3.1. Chemical and structural characterization of the reduced GO electrodes

Initially, the electrochemical reduction of the GO films was carried out by cyclic voltammetry in aqueous solutions between −1.5 and 0.1 V (*vs* Ag/AgCl/NaCl 3 M). The voltammetric curves in aqueous solution at pH 2 and 12 are shown in Fig. 1 for

several sweep cycles; the response of the bare steel collector is also shown for clarity. As seen, the steel current collector presented a very low current in the potential range from 0.1 to −1.1 V; the cathodic current gradually increased at more negative potentials up to −1.5 V, which is associated to the decomposition of the electrolyte. In contrast, the voltammetric curves of the GO coated electrodes displayed a marked capacitive character compared to the steel collector, corroborating the presence of the GO deposit. Also, the onset of the cathodic current shifted to slightly more positive potentials (*ca.* −0.8 and −1.0 V at pH 2 and 12, respectively).

The electrochemical reduction of the GO electrodes was evidenced by the gradual increase in the current density of the voltammograms with the number of cycles, indicating an increasing capacitive behavior of the electrodes. Furthermore, clear differences were observed depending on the pH of the electrolyte. In basic medium (Fig. 1b), two ill-defined waves were seen after the second cycle of potential sweep: a cathodic one at *ca.* −1.2 V and an anodic wave at *ca.* −0.7 V. It should be mentioned that the cathodic peak at −1.2 V was not observed during the first cycle of the cathodic sweep (see Fig. S1 in the Supplementary Information); it only appeared after reaching the potentials of the anodic wave (the applied potential sweep started in the cathodic direction from −0.1 V). This confirms that both redox reactions are linked, and that the reduced form of the electroactive pair is present in the pristine GO material. With every subsequent cycle (after the 2nd cycle) the peak potential difference between them (ΔE_p) increased, while the intensity of the waves decreased showing a *quasi*-reversible nature. The decrease in the intensity of the reduction wave at −1.2 V has been associated to the electrochemical reduction of GO [25]. After 15 cycles, neither changes in the shape, intensity nor peak potential were any longer considerable, indicating no further reduction of GO [26]. Another indicator of the reduction of GO is the cathodic current leap observed below −1.5 V *vs.* Ag/AgCl/NaCl 3 M; this is related to the electrochemical decomposition of the aqueous electrolyte to form nascent hydrogen, that is gradually shifted down to more negative potential values, as expected for a more reduced graphene oxide [27,28].

On the other hand, in acidic aqueous electrolyte (Fig. 1a) the voltammograms showed a less marked capacitive character (*i.e.* lower current densities); the anodic humps at −0.7 V were also less pronounced, while its corresponding reverse cathodic peak at −1.2 V was not detected in the reverse scans. The latter is an indicator that the O-groups in GO could undergo electron transfer reactions coupled to chemical reactions with H^+ at the electrode/electrolyte interface. The hydrogenation of the cation radical, electrogenerated during the anodic scan, would form a new −OH moiety, following a similar mechanism reported for the protonation of electrochemically reduced quinones in the presence of a H^+ donor [29]. According to the characterization of the films, the coupled chemical step does not affect the extent of the electrochemical reduction of O-groups in the GO electrode; in fact, it could be a necessary step for the removal of the groups. According to this, the electrochemical reduction of GO should display a faster kinetic in an acid electrolyte due to the higher concentration of H^+. This was further confirmed by recording the chronoamperometric response (Fig. 2) of the GO electrodes for the electrochemical reduction at −1.2 and −1.5 V, both in acidic and basic aqueous electrolytes.

As seen, the changes in current related to the reduction of the electrode material (*e.g.* depression in the curve) were achieved at shorter times in acid medium, regardless the applied potential. Interestingly, the time difference in basic medium is less marked if the applied potential is negative enough to electrolyze water and produce nascent hydrogen (*i.e.*, more negative than −1.2 V). The water electrolysis is evidenced by an increase in the cathodic

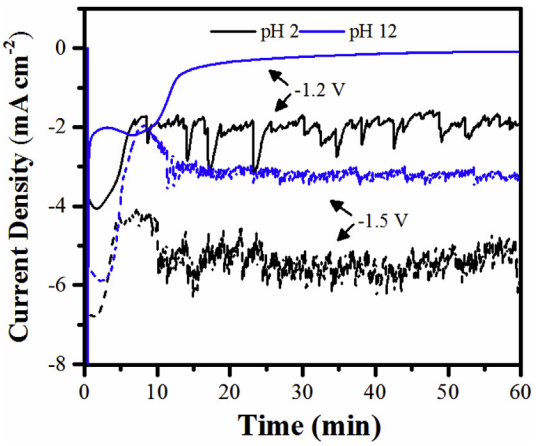

Fig. 2. Chronoamperometric curves obtained after applying half-cell potentials of −1.2 and −1.5 V to the GO electrode casted on the steel collector in both acid and basic electrolytes (argon saturated solutions, room temperature). (A colour version of this figure can be viewed online.)

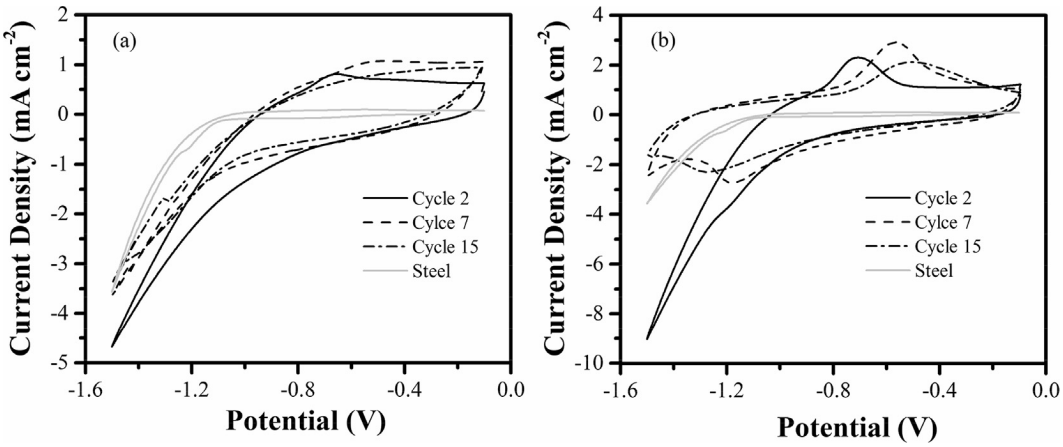

Fig. 1. Cyclic voltammetry of GO films casted on a steel collector in PBS solution at (a) pH 2 and (b) pH 12 (scan rate 20 mV s^{-1}, argon saturated solution, room temperature).

current after 9 min and by the fluctuations in current due to the gas evolution at −1.5 V, in basic and acid media, and at −1.2 V in acidic pH.

To corroborate the different reduction pathways, the electrodes were characterized after the electrochemical reduction using FTIR spectroscopy. Fig. 3 shows the corresponding spectra after 15 cycles of potential sweep in different electrolytes. In acid and basic aqueous electrolytes, the bands related to the bending and stretching vibrations of −OH bonds (*i.e.* hydroxyl groups and intercalated water between rGO sheets) at 3000-3700 cm^{-1} clearly decreased after the electrochemical treatment. The bands associated to epoxide groups (*ca.* 850 and 1170 cm^{-1}) also disappeared, whereas those associated to C═O (*ca.* 1720 cm^{-1}) and C—O in carboxylic moieties (*ca.* 1081 cm^{-1}) were still detected. This suggests that the first step in the reduction of GO at −1.2 V is a hydrogenation reaction, mainly of epoxide groups, resulting in the creation of hydroxyl groups that are removed upon subsequent cycles in the form of water. This contrasts with previous studies in the literature reporting the reduction of epoxide groups to alcohols and aldehydes (inferred from the increase in the band associated to −OH) when the electrochemical reduction is hold at −1 V, under similar experimental conditions [16]. Our results show that more negative cut-off potentials are needed to promote the further reduction of the hydroxyl groups.

Interestingly, the band associated to C═C stretching vibrations of hybridized sp^2 carbons (~1580 cm^{-1}) was less pronounced after the reduction of GO upon 15 cycles. Moreover, the bands at 2850 and 2920 cm^{-1} characteristic of the stretching vibrations of C—H in sp^3 bonds were detected in all the reduced samples, which shows the hydrogenation of carbon atoms. This effect seemed to be more pronounced in the aqueous electrolyte at acidic pH.

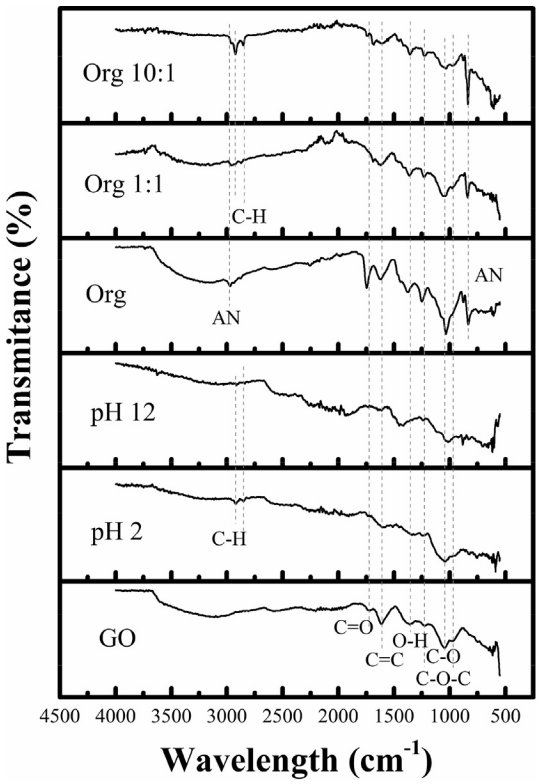

Fig. 3. FT-IR spectra of the pristine GO and the rGO films obtained after electrochemical reduction by applying 15 cycles of potential scan in the range from −0.1 to −1.5 V *vs* Ag/AgCl/NaCl 3 M using different electrolytes.

All this confirms that the electrochemical reduction of GO does not necessarily render materials with a complete sp^2 hybridization. Indeed, the removal of the O-groups located at the edges of the graphene-like domains generates carbon atoms with dangling bonds characterized by a high reactivity [30,31], which could subsequently undergo hydrogenation reactions. For the case of epoxide groups, located inside the graphene-like layers, the electrochemical reduction promotes the formation of hydroxyl groups, and further hydrogenation reactions would lead to the formation of defects in the graphene-sheets, consisting of sp^3 domains. These defects formed *via* electrochemical reduction reactions are expected to be different from those formed upon thermal and/or chemical reduction treatments, where the stabilization of the dangling bonds proceeds via oxygen chemisorption and/or polycondensation of carbon atoms in dense aromatic structures, generating vacancies [2,4].

For the electrochemical reduction of GO in organic electrolyte, phthalic acid was added as a proton donor in two different concentrations, namely meq proton donor:meq acceptor O-groups, ratios of 1:1 and 10:1. These ratios were calculated considering the amount of O-groups in the pristine GO quantified by Boehm titration (*ca.* 4.5 ± 0.4 meq g^{-1}) [23]. Fig. 4 shows the voltammetric responses of the GO electrodes after 15 cycles in the organic electrolyte in the presence (ratio 1:1 and 10:1) and absence of proton donor. The shapes of the voltammograms are different than those obtained in aqueous media (Fig. 1). All of them showed one broad cathodic wave in the first cycle of the potential sweep starting at *ca.* −0.85 V that disappeared upon cycling. Consecutive cycles also showed an increase in the capacitive current, as well as a pseudocapacitive redox process at *ca.* −0.9 V (cathodic peak) and −0.6 V (anodic peak). At a high proton donor ratio (*ca.* 10:1), a cathodic peak at −0.65 V was also observed in the first cycle (Fig. 4c). The origin of this peak remains unknown, but it could be attributed to a redox process involving O-groups that would be favored at high proton donor concentrations. This assumption is based on the observation that the broad cathodic wave (*ca.* ~ −1.4 V in the proton-free organic electrolyte) shifts to more positive values (*ca.* −1.3 ~ −1.2 V) when the proton donor is added to the electrolyte, which is again a clear indicator that the presence of an H^+ donor facilitates the reduction process.

The FTIR spectra of the samples reduced in organic electrolytic medium (Fig. 3) revealed that the bands at 2850 and 2920 cm^{-1} related to C—H bonds are only observed when the proton donor was added to the organic electrolyte. Compared to the films reduced in aqueous electrolytes, the band associated to the C═C stretching vibrations of hybridized sp^2 carbons (~1580 cm^{-1}) was less affected in the organic electrolyte, regardless the presence of the proton donor. Additionally, two bands featuring at 3000 and 800 cm^{-1} (labelled as AN) appeared in the FTIR spectra after the reduction in organic electrolyte. They are attributed to residual acetonitrile (solvent) or PF_6^- remaining in the electrodes [18].

The electrochemical reduction of the GO electrodes was further investigated by XPS. Figs. 5 and 7 show the high-resolution spectra of C1s and O1s core energy levels of the GO reduced in different electrolytic medium, respectively. The binding energy profile of C1s spectra were deconvoluted to various contributions (Table 1): carbon to carbon bonds in sp^2 (~284 eV) and sp^3 configurations (~284.8 eV); C—O single bond (~286 eV) assigned to phenolic, alkoxy, epoxydes and ether configurations; C═O double bond (~287 eV) assigned to carboxylic and carbonyl groups, and O—C═O bonds in carboxylic, ester groups (~288 eV). For the samples reduced in aqueous media (Fig. 5b and c), the spectra also showed broad peaks at 292.5 and 295 eV, associated to $K2p_{3/2}$ and $K2p_{1/2}$ signals from the residual potassium from the PBS solution. These peaks were not considered for further analysis.

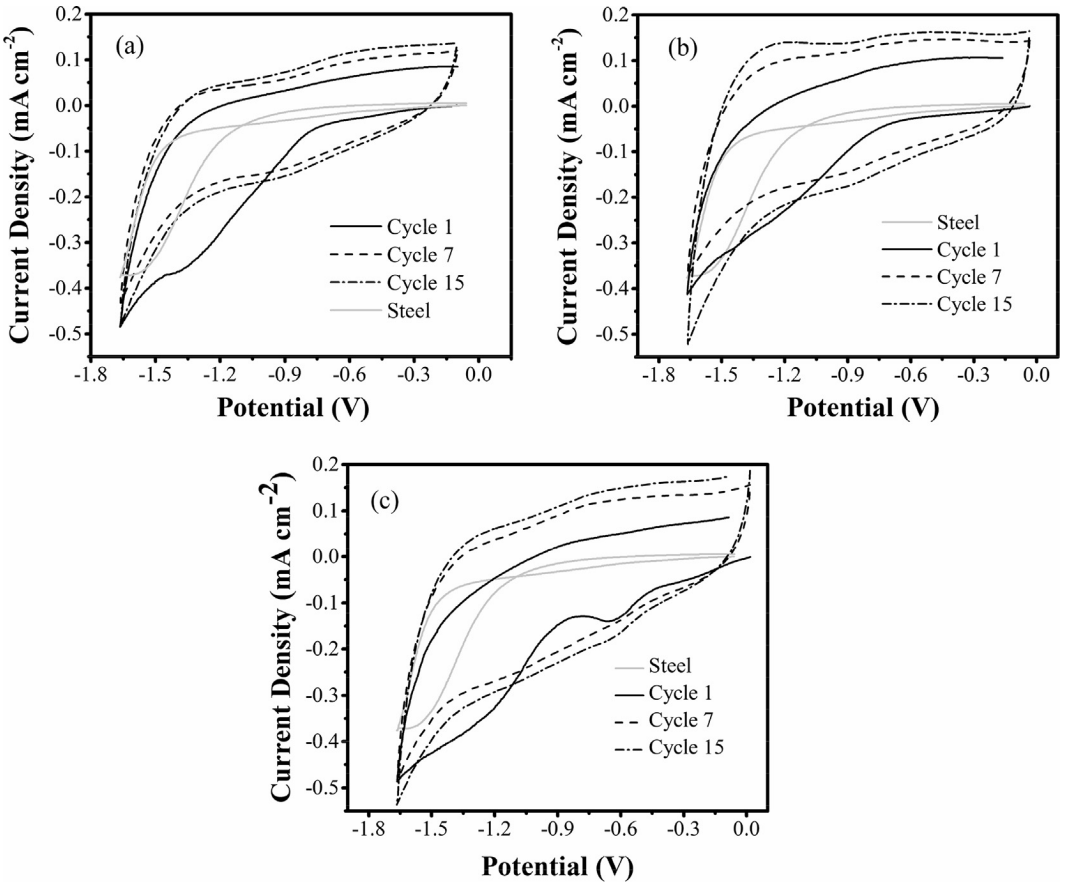

Fig. 4. Voltammetric responses of the rGO films obtained during the electrochemical reduction of GO in organic electrolyte with different proton donor to O-groups ratio: (a) 0:1, (b) 1:1 and (c) 10:1.

As seen, the electrochemical reduction affects mainly the C—O bonds (~286 eV) associated to epoxides and hydroxyl groups, and the C═O bonds (~287 eV) associated to carbonyl groups, regardless the nature of the electrolyte. This is in agreement with the observations from FTIR spectra. Fig. 6 shows that the electrochemical reduction in aqueous electrolytes leads to a material with higher atomic percentage of carbon to oxygen (*ca.* C/O) and carbon to carbon bonded to oxygen (C/C···O) ratios. This indicates a more efficient reduction of the pristine GO in aqueous electrolyte (*i.e.*, with a higher C/O ratio). Regarding the aqueous electrolytes, basic conditions lead to a material with a lower amount of O-groups and a higher abundance of carbon atoms in sp^2 configuration. Kauppila et al. [13] studied the electrochemical reduction of GO in acid and basic electrolytic solutions, reporting a C/O ratio of 3.4 and 2.0, respectively, when applying a potential of −0.71 V *vs* Ag/AgCl. However, at a more negative potential of −1.4 V, a C/O ratio of 4.10 was obtained in basic media. When comparing their results with ours, it can be seen that the C/C···O ratios obtained in acid media in this study are similar, even though the potential applied is quite different. This observation indicates that it is not necessary to reach too negative potentials in acidic medium (*e.g.*, −1.5 V) to reduce GO, since the reaction is favored in high concentrations of protons. However, in basic conditions, the removal of the O-groups is enhanced when the potential is negative enough to electrolyze water (*ca.* −1.5 V). Under such conditions, the obtained materials displayed higher C/O and C/C···O ratios than those reduced at acid pH. The latter may be explained due to the higher reactivity of the nascent hydrogen produced during water electrolysis in basic conditions; indeed, the nascent hydrogen generated at the interface GO/electrolyte would diffuse faster towards the GO surface than the H^+ in the bulk electrolyte.

It should be mentioned that the abundance of carbon to carbon bonds in sp^3 hybridization is non-negligible for any of the samples, indicating that the aromatization of the graphene-like layer is not complete upon the electrochemical reduction, and thus some defects are present in the rGO materials. Moreover, despite the high reduction efficiency achieved in acid aqueous electrolyte (inferred by a high C/C···O ratio) it also presented the lowest sp^2/sp^3 ratio (Fig. 6). The latter is an indicator of the key role of H^+ during the electrochemical reduction of GO. The presence of H^+ in the electrolyte favors the removal of oxygen groups *via* consecutive hydrogenation reactions; however, these reactions also seem to introduce defects consisting of sp^3 domains due to the hydrogenations of edge zones and/or dangling bonds created after the removal of O-groups located both in the edges and basal planes.

The latter becomes more evident when analyzing the data of the electrochemical reduction in organic electrolyte. As seen, the contribution of the peak related to carbon to carbon bonds in a sp^3 configuration decreased (accounting for *ca.* 20% abundance) achieving a higher sp^2/sp^3 ratio in comparison to aqueous electrolyte at acid pH. However, the abundance of carbon atoms bonded to oxygen is still high compared to aqueous media. In the organic electrolyte, due to the absence of a proton donor, hydrogenation of the sp^2 domains is not expected, thus the electrochemical reduction proceeds through the removal of oxygen functionalities without the stabilization of the reactive edges *via* C—H bonds.

Fig. 7 shows the O 1s core level signal of the studied samples, decomposed in three peaks associated to C—O (~532.3 eV), C═O

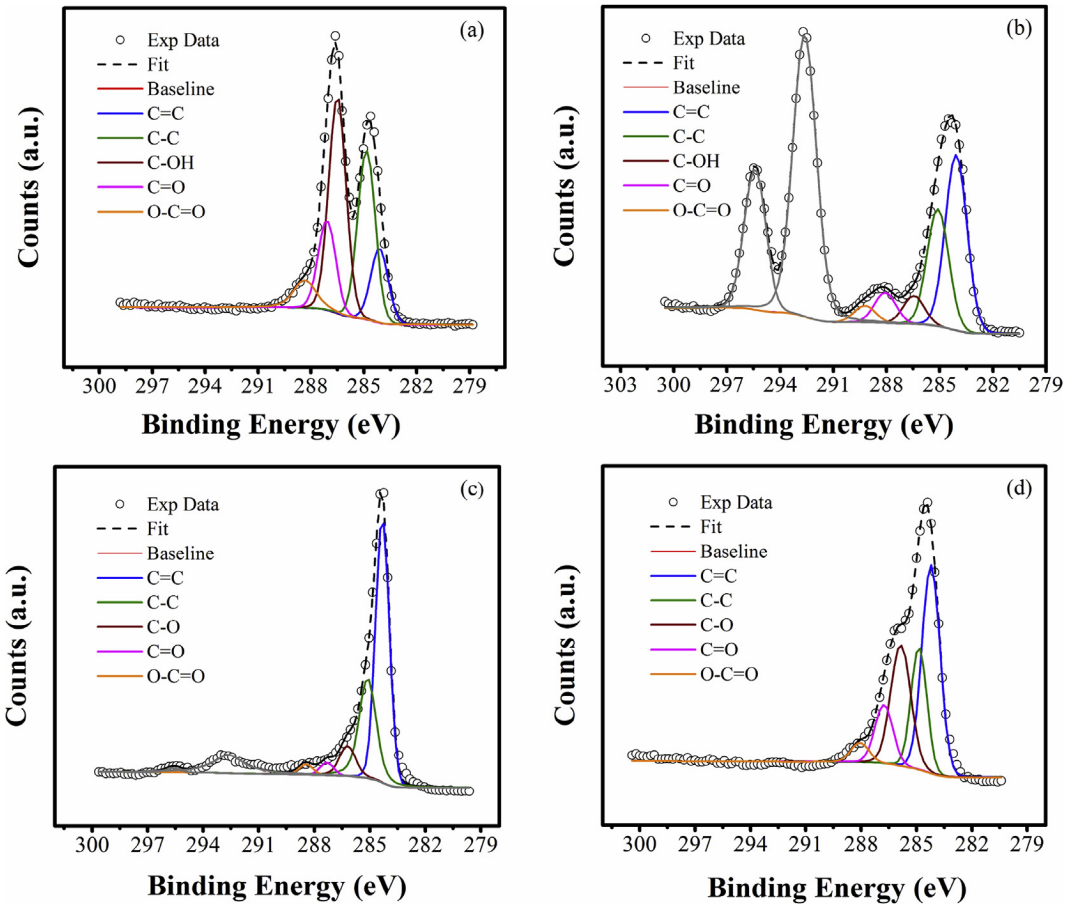

Fig. 5. High resolution XPS spectra of the C1s peak of the pristine and reduced materials obtained by electrochemical reduction with 15 cycles of potential scan in the potential range from 0.1 to −1.5 V *vs* Ag/AgCl/NaCl 3 M in different electrolytes: (a) pristine GO; b) aqueous electrolyte at pH 2, (c) aqueous electrolyte at pH 12, (d) organic electrolyte. (A colour version of this figure can be viewed online.)

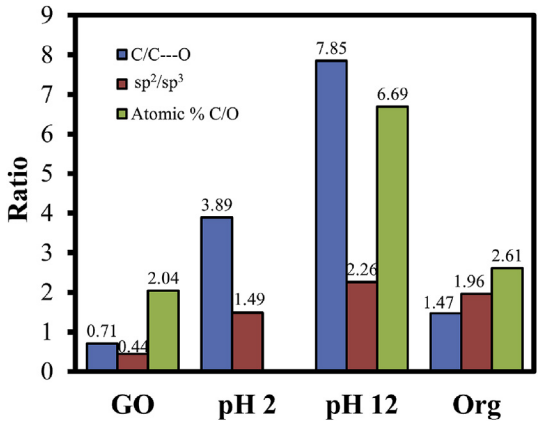

Fig. 6. Relative abundance of carbon and oxygen species estimated from XPS data upon evaluation of C/O ratio, sp^2/sp^3 ratio and C/C···O ratio in the pristine GO and the rGO obtained after electrochemical reduction in aqueous electrolyte at pH 2 and pH 12 and in organic electrolyte (Org). (A colour version of this figure can be viewed online.)

(~531.2 eV), and O–C=O bonds (~533.6 eV). As seen, there is a marked reduction in the C–O and C=O contributions of all the samples, in agreement with the trends observed in the C1s core level. Additionally, the amount of oxygen in the samples followed the trend: GO (33 at.%) > rGO reduced in the proton-free organic electrolytic solution (28 at.%) > rGO reduced at pH 12 (13 at.%), indicating one more time that the removal of O-groups in GO is more efficient in aqueous medium if H^+ or nascent hydrogen are available.

The occurrence of structural changes upon the electrochemical reduction was analyzed by Raman spectroscopy (Fig. S2). For all the studied samples, the characteristic G and D bands in the region between 1000 and 2000 cm^{-1} were observed as the main features. The G band located around 1595 cm^{-1} is assigned to allowed E_{2g} transitions resulting from 'in-plane' displacement of carbons strongly coupled in the hexagonal sheets modes (*i.e.*, defect-free graphitic domains). The D band, around 1355 cm^{-1}, is associated to the breathing mode A_{1g} of 6-member carbon rings and active in disordered materials with short-range translation symmetry. Hence, it can be associated to the presence of defects in GO, such as vacancies or oxygenated groups [32,33].

The variation of the I_D/I_G ratio is a useful measure of any changes in the structural ordering of a carbon network. We have herein used this parameter as an indicator of the degree of reduction of GO and as an indicator of the introduction of more defects in the material [8,15,34]. As seen in Fig. 8, the I_D/I_G ratio of pristine GO (*ca.* 0.87) increased significantly after the electrochemical reduction in aqueous solutions (*ca.* 1.43 and 1.2 for the aqueous electrolyte at pH 2 and 12, respectively), as opposed to the behavior in the proton-free organic medium (*ca.* 0.80). Furthermore, when a proton donor was added to the organic electrolyte, the I_D/I_G ratio of the reduced samples showed a slight increase with the amount of proton donor; nevertheless, the values were still lower than those

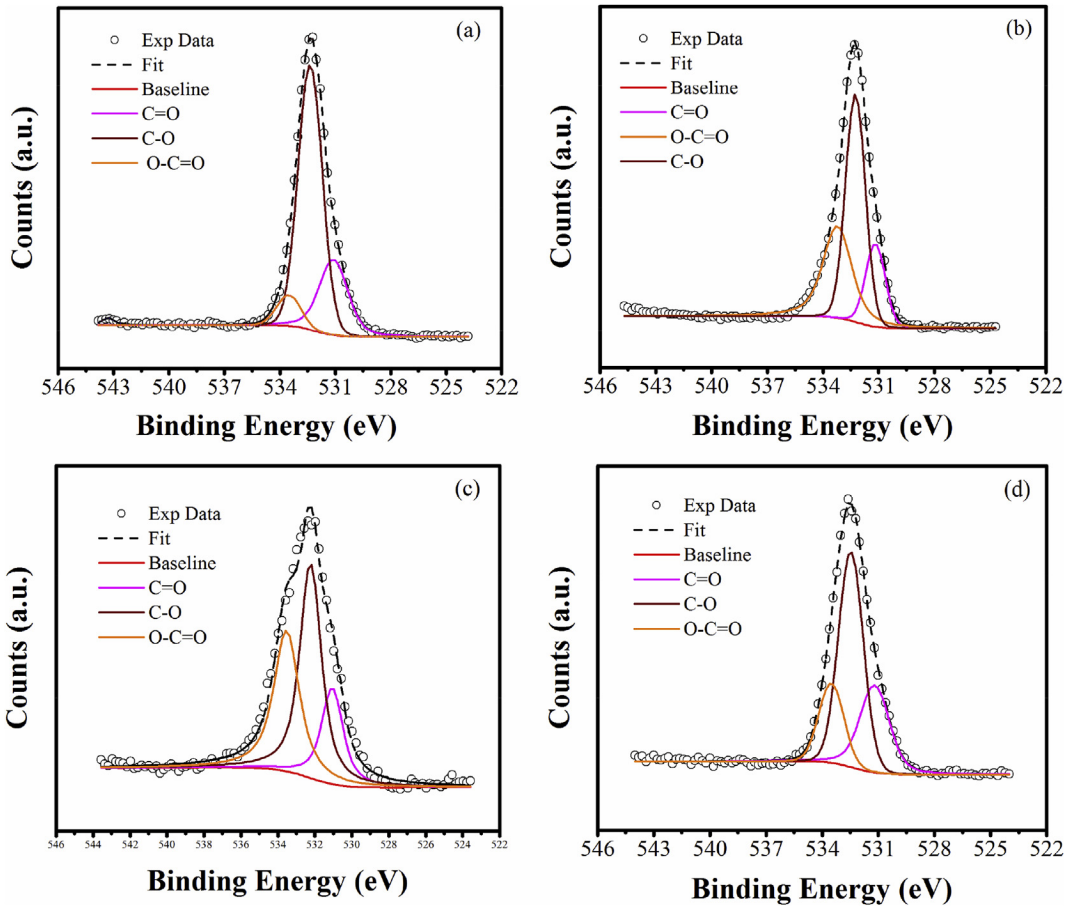

Fig. 7. High resolution XPS spectra of the O1s peak of the pristine and reduced materials obtained by electrochemical reduction with 15 cycles of potential scan in the potential range from 0.1 to −1.5 V *vs* Ag/AgCl/NaCl 3 M in different electrolytes: (a) pristine GO; b) aqueous electrolyte at pH 2, (c) aqueous electrolyte at pH 12, (d) organic electrolyte. (A colour version of this figure can be viewed online.)

Table 1
Relative abundance (%) of the different peaks assigned from the deconvolution of the C1s and O1s core energy levels for the pristine GO, and the rGO after electrochemical reduction in aqueous electrolyte at pH 2 and 12, and in organic electrolyte (Org).

	C1s					O1s		
Sample	C sp^2	C sp^3	C–O	C=O	O–C=O	C=O	C–O	O–C=O
GO	12.7	28.7	36.7	15.1	6.8	25.2	67.0	7.8
pH 2	47.7	31.9	7.7	8.2	4.6	17.6	48.5	33.8
pH 12	61.5	27.2	7.0	2.4	1.9	19.9	44.7	35.5
Org	39.4	20.2	25.6	11.1	3.7	28.0	52.6	19.5

of the pristine GO, indicating that the amount of proton donor added was not enough to drive important structural changes in the material. An increase in the I_D/I_G ratio has often been attributed to a high density of sp^2 domains of small sizes due to the introduction of defects of varied nature (*e.g.*, vacancies, functionalization, aromatic structures other than 6-membered units) [8]. Since the increase in the I_D/I_G ratio was accompanied by an increase in the sp^3 domains (as inferred by XPS data), we consider this evidence as a direct indicator of the presence of defects consisting in sp^3 domains introduced during the electrochemical reduction of GO in aqueous electrolytes when H^+ are available. The electrochemical characterization also supports this correlation, as it will be discussed below. Furthermore, it should be mentioned that the complete hydrogenation of all the carbon atoms initially bonded to an O-group is not likely to occur, as the resulting rGO material would

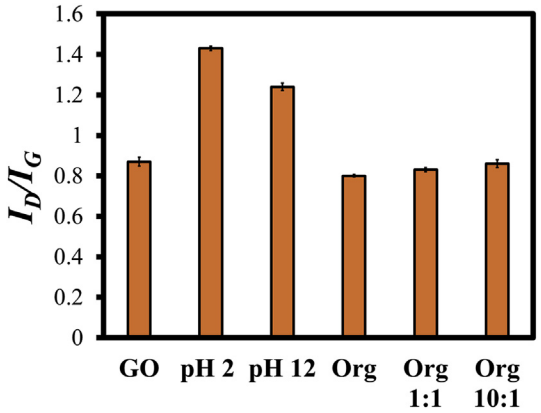

Fig. 8. I_D/I_G ratio obtained from the Raman spectra of the pristine and reduced materials after 15 cycles of potential scan in the potential range from 0.1 to −1.5 V *vs* Ag/AgCl/NaCl 3 M in different electrolytes: pristine GO; aqueous electrolyte at pH 2 and 12; and organic electrolyte (Org) in the absence and presence of proton donor (1:1 and 1:10 ratio). (A colour version of this figure can be viewed online.)

be an insulator just as GO, and the electrochemical features of the rGO materials discussed below, show that this was not the case for herein studied materials.

Summarizing, all the characterization techniques confirmed that the electrochemical reduction in aqueous medium renders a

defective material regardless the pH of the solution (in basic medium, the applied potential needs to be negative enough to electrolyze water and produce nascent hydrogen for the compliance of the latter statement). The concentration of protons in the electrolytes at the beginning of the experiments corresponds to proton:O-groups ratios of 54:1 and 4×10^{-7}:1, for pH 2 and 12, respectively. However, both ratios can shift due to water electrolysis and hydrogen reduction in basic and acid pH.

To acquire more information about the mechanism of the electrochemical reduction of GO, various constant potential values were applied during different times and the resulting electrodes were characterized by Raman spectroscopy (Fig. 9). As seen, regardless the applied potential and the polarization time, when the electrochemical reduction was carried out in the proton-free organic electrolyte, the rGO materials presented a lower modification of the structural parameters (lower I_D/I_G values than in the pristine GO). In contrast, a higher modification of the structural parameters was observed when the electrochemical reduction was carried out in an aqueous electrolyte. Regardless the applied potential, a high concentration of protons (pH 2) facilitates the electrochemical reduction of GO and the introduction of defects (*i.e.*, high I_D/I_G ratio). Even at the lowest potential values and the shortest polarization times, the reduced material displayed a relatively high I_D/I_G ratio. On the other hand, the materials reduced in basic pH electrolyte at −0.8 V *vs* Ag/AgCl/NaCl 3 M (potential not negative enough to electrolyze water) showed lower I_D/I_G ratios. This could be attributed to the lower efficiency of removal of the O-groups in basic pH and, therefore, less defects are introduced. Only when the applied potential was negative enough to electrolyze water and generate nascent hydrogen (*ca.* −1.2 V and below) the I_D/I_G ratio were similar to those of the materials reduced at acidic pH.

3.2. Electrochemical properties of the reduced GO electrodes

The changes in the electrochemical properties of the GO after the electrochemical reduction in different conditions were evaluated in 0.5 M Na_2SO_4 as inert electrolyte and using the ferricyanide redox probe.

Fig. 10 shows the voltammetric response of the rGO materials in 0.5 M Na_2SO_4. As seen, the area of the voltammograms was higher for the samples reduced in aqueous electrolytes. The capacitance of the electrodes was estimated from the voltammograms (Fig. 10 inset), showing higher values for the rGO films reduced in basic media, followed closely by the capacitance of the films reduced in acid medium. For the materials reduced in organic medium, no significant differences were obtained regarding the proton donor concentration. Since a linear correlation is expected between the reduction degree (C/O ratio) of GO and its capacitance, this suggests that the electrochemical reduction in aqueous media is achieved to a larger extent than in an organic electrolyte [35].

Fig. 11 shows the voltammetric response of the electrodes in the ferricyanide redox probe. Data of the bare current collector after 15 potential cycles in the corresponding electrolytic solution is also shown for comparison. After the electrochemical reduction in aqueous media, the peaks corresponding to the electron transfer of the ferricyanide became broad and ill-defined. Additionally, the ΔE_p between the anodic and cathodic peak increased in the reduced samples, indicating a slower electron transfer. Indeed, ΔE_p values of 0.318 and 0.246 V were obtained for the samples reduced at pH 2 and 12, respectively. This confirms that the rGO presented a

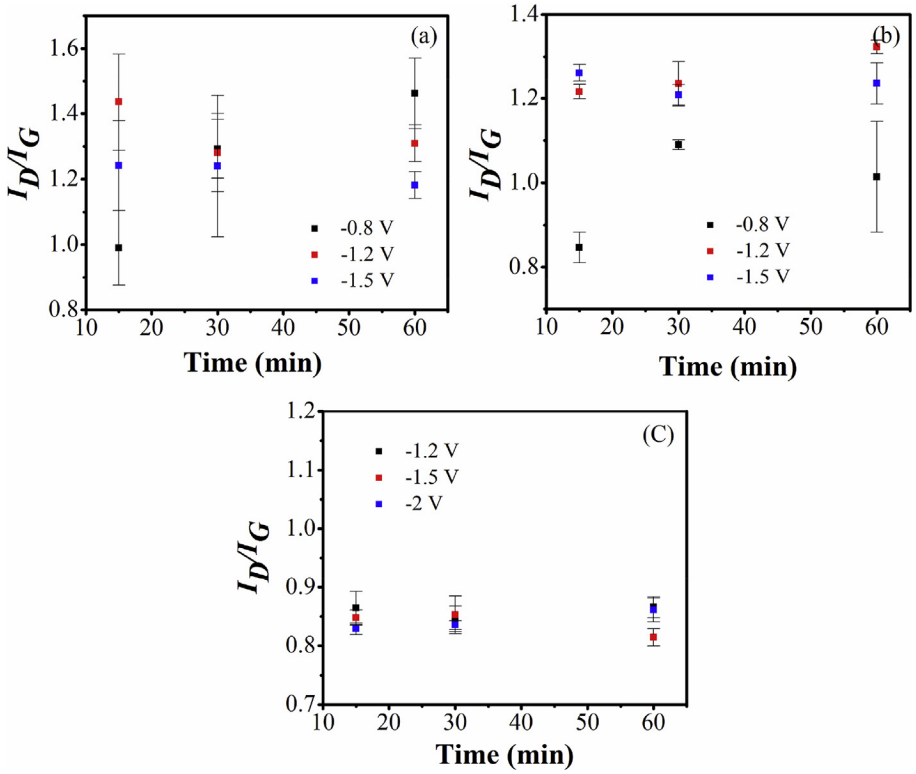

Fig. 9. I_D/I_G ratio obtained from the Raman spectra of the pristine and reduced materials after applying different constant potential values during different times, in different electrolytes: (a) aqueous electrolyte at pH 2; (b) aqueous electrolyte at pH 12; (c) proton-free organic electrolyte. (A colour version of this figure can be viewed online.)

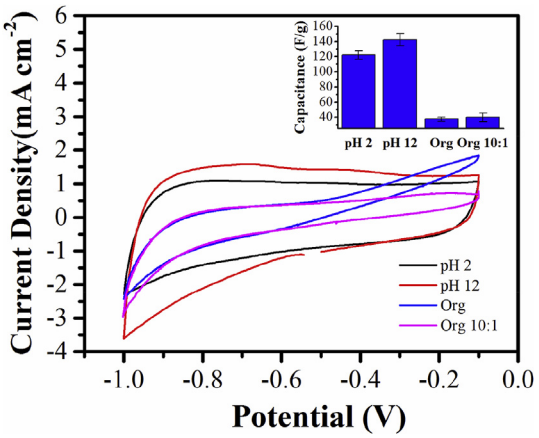

Fig. 10. Cyclic voltammetries in 0.5 M Na_2SO_4 of the rGO materials prepared after the electrochemical reduction using 15 cycles of potential scan in the potential range from 0.1 to −1.5 V *vs* Ag/AgCl/NaCl 3 M in different electrolytes: aqueous electrolyte at pH 2 and 12, proton-free organic electrolyte (Org) and organic electrolyte with proton donor ratio of 10:1 (scan rate 10 mVs^{-1}, argon saturated solutions, room temperature). (A colour version of this figure can be viewed online.)

high resistivity, attributed to the presence of the sp^3 domains formed by the hydrogenation reactions. This is in agreement with the data from the XPS spectra (Figs. 5 and 6), as the abundance of carbon atoms in sp^3 hybridization is higher in the sample reduced at pH 2. In the proton-free organic electrolyte, the ferricyanide pair exhibited a more reversible character, with a ΔE_p value close to 0.138 V. This value is smaller than those obtained for the samples reduced in aqueous media (Fig. 11a and b) despite a less efficient reduction (based on the C/O and C/C···O ratios). This may be due to the lower contribution of sp^3 domains of the samples as shown in the XPS data (Figs. 5 and 6), attributed to the absence of hydrogenation reactions. Interestingly, the current density values of the rGO samples reduced in the organic electrolyte were 10 times smaller than those reduced in aqueous solutions. This could be attributed to the presence of O-groups remaining in the rGO (since the overall reduction reaction is less efficient). Nevertheless, the contribution of the passivation of the gold current collector during the cathodic cycling (Fig. 11c) cannot be discarded.

All this demonstrates that a careful selection of the H^+ concentration should be done so as to control the electrical conductivity of the obtained rGO material. It is important to stress on this result, because it demonstrates the importance of knowing the nature of defects created during the reduction of GO. For an intended application, C/O ratios could not be as important as the density of defects (for example an electrochemical sensor of Fe ions), thus precautions should be taken to control the (un)necessary introduction of defects in the material, *vs* an efficient removal of O-groups.

The defects created by the electrochemical reduction method are, in fact, different than those caused by other reduction protocols such thermal (*e.g.*, vacancies) [4] or chemical (*e.g.*, functionalization) reduction [2]. As a result, the reactivity of the rGO films is different. For instance, we have reported the performance, as anticorrosive coatings for carbon steel, of rGO films produced by electrochemical reduction [23] and compared those results with a

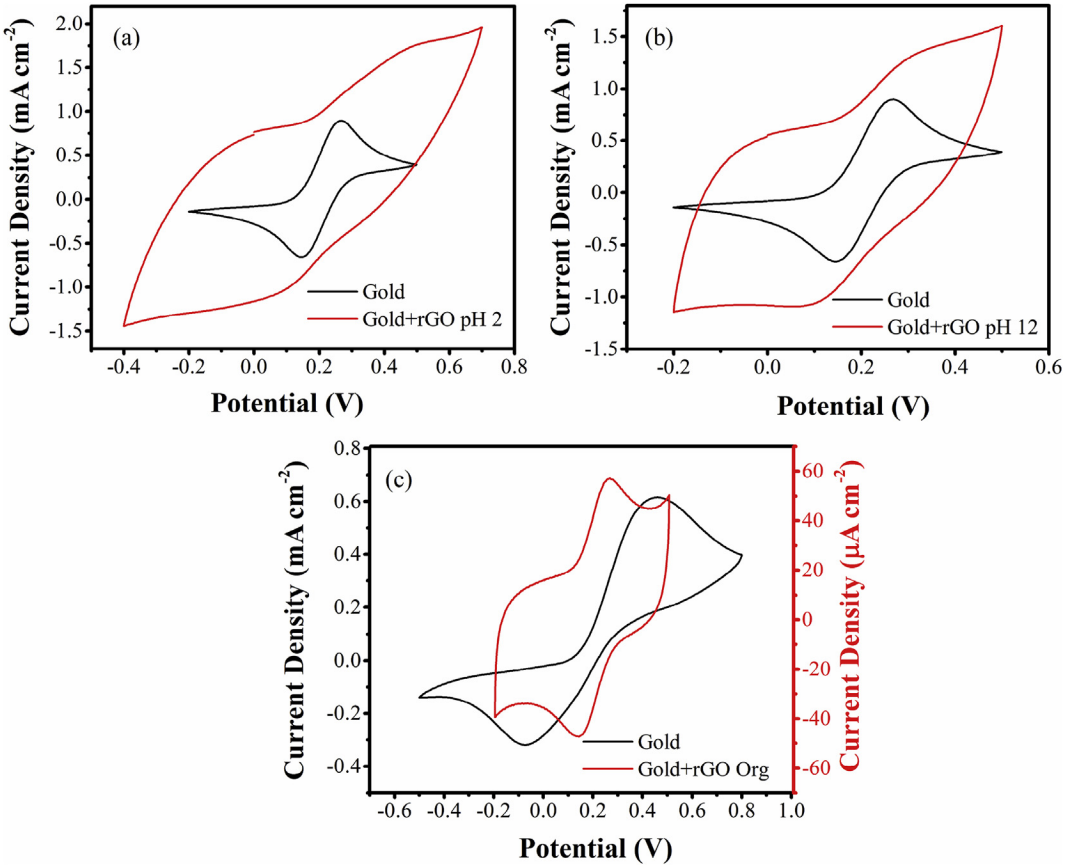

Fig. 11. Voltammetric response of 0.01 M $K_4[Fe(CN)_6]$ in 0.1 M PBS solution over rGO samples prepared after 15 cycles of potential scan in the potential range from 0.1 to −1.5 V *vs* Ag/AgCl/NaCl 3 M in different electrolytes: (a) aqueous electrolyte at pH 2; (b) aqueous electrolyte at pH 12; (c) proton free organic electrolyte (scan rate of 20 mV s^{-1}, argon saturated solution, room temperature). (A colour version of this figure can be viewed online.)

film produced using electrochemical oxidation to remove O-groups in the form of CO_2 [36]. The rGO film produced by electrochemical reduction outperformed the one produced by electrochemical oxidation, despite the higher number of defects (in terms of I_D/I_G ratio) of the former. This behavior can be attributed to the difference in the defects of both rGO; the removal of O-groups by electrochemical oxidation may cause vacancies and polycondensation of carbon atoms in dense aromatic structures [37], as opposed to the defects introduced during the electrochemical reduction of GO, mainly consisting in sp^3 domains caused by the hydrogenation of dangling bonds and reactive zones like edges. This particular type of defects are suitable for the application of the rGO as an anti-corrosive coating, due to the lower reactivity, enhanced hydrophobicity and to the fact that they don't compromise the impermeability property of graphene sheets (unlike vacancies caused by the removal of O-groups in the form of CO_2).

4. Conclusions

This work shows the critical role of H^+ in the electrochemical reduction of GO. The presence of protons in aqueous electrolytes facilitates the removal of oxygen functionalities and simultaneously causes the hydrogenation of the carbon atoms in the graphitic domains. These reactions can also occur in basic pH conditions in aqueous medium if the applied potential is negative enough, and/or applied long enough, to electrolyze water and produce nascent hydrogen. The C/O ratio of the rGO samples followed the trend pH 12 > pH 2 > organic electrolyte, indicating the better efficiency of aqueous electrolytes for the removal of O-functionalities. However, the samples reduced in acidic electrolyte showed the lowest sp^2/sp^3 ratio, corroborating the introduction of defects consisting on sp^3 domains caused by the hydrogenation of high reactivity zones in the graphitic sheets. Thus, the concentration of H^+ in the electrolyte can be used to obtain rGO with *ad-hoc* characteristics, which has a strong impact on performance of the resulting rGO materials. The contribution of this work lays on the importance of knowing the nature of defects introduced during the electrochemical reduction of GO; particularly since depending on the application, tuning the C/O ratio may not be as important as controlling the density of defects. The latter was evidenced by the ferrocyanide redox-probe, where the materials reduced in organic electrolyte outperformed those produced in aqueous electrolytes (with higher C/O ratios). Further research is still needed to unravel when the hydrogenation reactions affect the graphitic domains during the electrochemical reduction in aqueous media, since this could be linked to the nature (chemistry) of the O-moiety itself, or its location in the edge/planes of the graphene sheets.

Acknowledgments

The authors would like to thank CONACYT for the PhD scholarship (grant 25840) and for the financial support (project SEP-CONACyT, 169634). COA thanks the European Research Councilfor financial support through a Consolidator Grant (648161, PHOR-OSOL). The technical support of Dulce Partida, Juan Pablo Rodas and Elizabeth Cortez, as well as Mariela Bravo-Sanchez and Beatriz Rivera from LINAN with XPS and Raman measurements is also acknowledged.

Appendix A. Supplementary data

Supplementary data to this article can be found online at https://doi.org/10.1016/j.carbon.2019.04.109.

References

[1] D.R. Dreyer, S. Park, C.W. Bielawski, R.S. Ruoff, The chemistry of graphene oxide, Chem. Soc. Rev. 39 (2010) 228–240.
[2] S. Pei, H.M. Cheng, The reduction of graphene oxide, Carbon 50 (2012) 3210–3228.
[3] R. Backreedy, J.M. Jones, M. Pourkashanian, A. Williams, A study of the reaction of oxygen with graphite, Model Chem. 119 (2001) 385–394.
[4] M. Acik, G. Lee, C. Mattevi, A. Pirkle, R.M. Wallace, M. Chhowalla, et al., The role of oxygen during thermal reduction of graphene oxide studied by infrared absorption spectroscopy, J. Phys. Chem. C 115 (2011) 19761–19781.
[5] X. Gao, J. Jang, S. Nagase, Hydrazine and thermal reduction of graphene Oxide : reaction mechanisms and design, J. Phys. Chem. C 114 (2010) 832–842.
[6] P.V. Kumar, N.M. Bardhan, G. Chen, Z. Li, A.M. Belcher, J.M. Grossman, New insights into the thermal reduction of graphene oxide : impact of oxygen clustering, Carbon 100 (2016) 90–98.
[7] A. Bagri, C. Mattevi, M. Acik, J.Y. Chabal, M. Chhowalla, V.B. Shenoy, Structural evolution during the reduction of chemically derived graphene oxide, Nat. Chem. 2 (2010) 581–587.
[8] S. Stankovich, D.A. Dikin, R.D. Piner, K.A. Kohlhaas, A. Kleinhammes, Y. Jia, et al., Synthesis of graphene-based nanosheets via chemical reduction of exfoliated graphite oxide, Carbon 45 (2007) 1558–1565.
[9] Y. Shen, T. Jing, W. Ren, J. Zhang, Z.G. Jiang, Z.Z. Yu, et al., Chemical and thermal reduction of graphene oxide and its electrically conductive polylactic acid nanocomposites, Compos. Sci. Technol. 72 (2012) 1430–1435.
[10] E. Tegou, G. Pseiropoulos, M.K. Filippidou, S. Chatzandroulis, Low-temperature thermal reduction of graphene oxide films in ambient atmosphere: infra-red spectroscopic studies and gas sensing applications, Microelectron. Eng. 159 (2016) 146–150.
[11] A. Ambrosi, M. Pumera, Precise tuning of surface composition and electron-transfer properties of graphene oxide films through electroreduction, Chem. A Eur. J. 19 (2013) 4748–4753.
[12] S.J. An, Y. Zhu, S.H. Lee, M.D. Stoller, T. Emilsson, S. Park, et al., Thin film fabrication and simultaneous anodic reduction of deposited graphene oxide platelets by electrophoretic deposition, J. Phys. Chem. Lett. 1 (2010) 1259–1263.
[13] J. Kauppila, P. Kunnas, P. Damlin, A. Viinikanoja, C. Kvarnström, Electrochemical reduction of graphene oxide films in aqueous and organic solutions, Electrochim. Acta 89 (2013) 84–89.
[14] S. Liu, J. Ou, J. Wang, X. Liu, S. Yang, A simple two-step electrochemical synthesis of graphene sheets film on the ITO electrode as supercapacitors, J. Appl. Electrochem. 41 (2011) 881–884.
[15] H.L. Guo, X.F. Wang, Q.Y. Qian, F.B. Wang, X.H. Xia, A green approach to the synthesis of graphene nanosheets, ACS Nano 3 (2009) 2653–2659.
[16] A. Viinikanoja, Z. Wang, J. Kauppila, C. Kvarnström, Electrochemical reduction of graphene oxide and its in situ spectroelectrochemical characterization, Phys. Chem. Chem. Phys. 14 (2012) 14003.
[17] M. Zhou, Y. Wang, Y. Zhai, J. Zhai, W. Ren, F. Wang, et al., Controlled synthesis of large-area and patterned electrochemically reduced graphene oxide films, Chem. A Eur. J. 15 (2009) 6116–6120.
[18] A. Viinikanoja, J. Kauppila, P. Damlin, M. Suominen, C. Kvarnström, In situ FTIR and Raman spectroelectrochemical characterization of graphene oxide upon electrochemical reduction in organic solvents, Phys. Chem. Chem. Phys. 17 (2015) 12115–12123.
[19] Y. Harima, S. Setodoi, I. Imae, K. Komaguchi, Y. Ooyama, J. Ohshita, et al., Electrochemical reduction of graphene oxide in organic solvents, Electrochim. Acta 56 (2011) 5363–5368.
[20] W.J. Basirun, M. Sookhakian, S. Baradaran, M.R. Mahmoudian, M. Ebadi, Solid-phase electrochemical reduction of graphene oxide films in alkaline solution, Nanoscale Res. Lett. 8 (2013) 397.
[21] H. Öztürk, D. Ekinci, Ü. Demir, Atomic scale imaging and spectroscopic characterization of electrochemically reduced graphene oxide, Surf. Sci. 611 (2013) 54–59.
[22] J.D. Roy-mayhew, I.A. Aksay, Graphene materials and their use in dye-sensitized solar cells, Chem. Rev. 114 (2014) 6323–6348.
[23] J.A. Quezada-Renteria, L.F. Chazaro-Ruiz, J.R. Rangel-Mendez, Synthesis of reduced graphene oxide (rGO) films onto carbon steel by cathodic electrophoretic deposition: anticorrosive coating, Carbon 122 (2017) 266–275.
[24] 2013-2018 Therrmo Scientific Inc, Thermo scientific XPS Simplified. https://xpssimplified.com/index.php. Accesed in October 2018.
[25] X. Zhang, D. Zhang, Y. Chen, X. Sun, Y. Ma, Electrochemical reduction of graphene oxide films: preparation, characterization and their electrochemical properties, Chin. Sci. Bull. 57 (2012) 3045–3050.
[26] Y. Shao, J. Wang, M. Engelhard, C. Wang, Y. Lin, Facile and controllable electrochemical reduction of graphene oxide and its applications, J. Mater. Chem. 20 (2010) 743–748.
[27] M. Biswal, A. Deshpande, S. Kelkar, S. Ogale, Water electrolysis with a conducting carbon cloth: subthreshold hydrogen generation and superthreshold carbon quantum dot formation, ChemSusChem 7 (2014) 883–889.
[28] P.K. Dubey, A.S.K. Sinha, S. Talapatra, N. Koratkar, P.M. Ajayan, O.N. Srivastava, Hydrogen generation by water electrolysis using carbon nanotube anode, Int. J. Hydrogen Energy 35 (2010) 3945–3950.
[29] X.Y. Peng, X.X. Liu, D. Diamond, K.T. Lau, Synthesis of electrochemically-reduced graphene oxide film with controllable size and thickness and its

use in supercapacitor, Carbon 49 (2011) 3488–3496.
[30] A. Ambrosi, C.K. Chua, A. Bonanni, M. Pumera, Electrochemistry of graphene and related materials, Chem. Rev. 114 (2014) 7150–7188.
[31] P.M. Hallam, C.E. Banks, Quantifying the electron transfer sites of graphene, Electrochem. Commun. 13 (2011) 8–11.
[32] A.C. Ferrari, J. Robertson, Interpretation of Raman spectra of disordered and amorphous carbon, Phys. Rev. B 61 (14) (2000) 295.
[33] F. Tuinstra, J.L. Koenig, Raman spectrum of graphite, J. Chem. Phys. 53 (1970) 1126–1130.
[34] R. Panigrahi, S.K. Srivastava, Selective reduction of graphite oxide: a novel approach, RSC Adv. 4 (2014) 53055–53059.
[35] L. Buglione, E.L.K. Chng, A. Ambrosi, Z. Sofer, M. Pumera, Graphene materials preparation methods have dramatic influence upon their capacitance, Electrochem. Commun. 14 (2012) 5–8.
[36] J.H. Park, J.M. Park, Electrophoretic deposition of graphene oxide on mild carbon steel for anti-corrosion application, Surf. Coating. Technol. 254 (2014) 167–174.
[37] M. Diba, A. García-Gallastegui, R.N. Klupp-Taylor, F. Pishbin, M.P. Ryan, M.S.P. Shaffer, et al., Quantitative evaluation of electrophoretic deposition kinetics of graphene oxide, Carbon 67 (2014) 656–661.